nature water

Article

https://doi.org/10.1038/s44221-023-00147-9

Apparent surface conductance sensitivity to vapour pressure deficit in the absence of plants

Received: 29 March 2023

Accepted: 18 September 2023

Published online: 16 October 2023

Check for updates

Lucas R. Vargas Zeppetello[1] ✉, Kaighin A. McColl[1,2] ✉, Jeremiah A. Bernau[3], Brenda B. Bowen[3,4], Lois I. Tang[1], N. Michele Holbrook[5], Pierre Gentine[6,7] & Peter Huybers[1,2]

A growing literature argues that ecosystem-scale evapotranspiration is more sensitive to drying of the atmosphere because of stomatal regulation by plants than to reductions in surface soil moisture. Past studies analysed observations, for which it is difficult to conclusively control for potential relations among plant physiology, measurable state variables such as vapour pressure deficit (VPD) or soil moisture, and ecosystem-scale water flux. Here we analyse natural mechanism-denial experiments at non-vegetated but hydrologically active salt flats. At these sites, any apparent sensitivity of the ecosystem-scale surface conductance (g_s, a bulk measure of how the land surface influences evapotranspiration) to VPD cannot be due to stomatal closure. Over the salt flats we find a VPD–g_s relation similar to that commonly attributed to stomatal closure, and reproduce similar relations using a parsimonious boundary layer model that excludes plants. We conclude that observational studies probably overstate the sensitivity of ecosystem-scale surface conductance to atmospheric drying and understate the importance of variations in surface soil moisture. This finding has broad implications for future ecosystems, because anthropogenic trends in soil moisture are uncertain and spatially heterogeneous whereas ubiquitous atmospheric drying is expected due to global warming.

Evapotranspiration (E), the rate at which moisture is transferred from the land surface to the atmosphere, exerts a fundamental control on continental climate[1]. Since the earliest attempts to model evapotranspiration numerically, aerodynamic and surface conductance parameters have been used to quantify the influence of various environmental forcings on this fundamental water and energy flux[2,3]. Because neither conductance can be measured directly, the different controls on evapotranspiration exerted by the atmosphere and the land surface must be inferred from observations. While formulae exist for aerodynamic conductance as a function of wind speed and atmospheric stability[4], the environmental controls on ecosystem-scale surface conductance are the subject of debate.

The debate centres on whether soil moisture or atmospheric vapour pressure deficit (VPD) has a greater role in the regulation of ecosystem-scale surface conductance. In the initial development of techniques for estimation of E from available observations, surface

[1]Department of Earth and Planetary Sciences, Harvard University, Cambridge, MA, USA. [2]School of Engineering and Applied Sciences, Harvard University, Cambdrige, MA, USA. [3]Department of Geology and Geophysics, University of Utah, Salt Lake City, UT, USA. [4]Global Change and Sustainability Center, University of Utah, Salt Lake City, UT, USA. [5]Department of Organismic and Evolutionary Biology, Harvard University, Cambridge, MA, USA. [6]Department of Earth and Environmental Engineering, Columbia University, New York, NY, USA. [7]Data Science Institute, Columbia University, New York, NY, USA. ✉e-mail: lzeppetello@fas.harvard.edu; kmccoll@seas.harvard.edu

conductance was understood to depend mainly on soil moisture, even in vegetated ecosystems[5,6]. In parallel, plant physiological studies demonstrated that stomatal (not surface) conductance varies as a function of atmospheric relative humidity and VPD[7–12]. More recent studies have extrapolated the stomatal conductance sensitivity to atmospheric dryness up to the ecosystem scale, and have used observations of VPD and soil moisture to argue that VPD is often a more dominant control on ecosystem-scale surface conductance than soil moisture[13–17]. Despite the empirical relation between stomatal conductance and VPD, Mott & Parkhurst[18] showed that stomata respond to water loss from plant tissue rather than by direct sensing of VPD. While stomata are known to respond to variations in soil water that impact water stress in plant tissue, the causal relation between VPD and surface conductance on cellular and ecosystem scales remains unclear[19].

Capturing the correct relation among VPD, soil moisture and ecosystem-scale surface conductance is important in regard to climate change projections, for two reasons. First, the projections of VPD and soil moisture are not equally well constrained. General circulation models are in nearly universal agreement that global warming will substantially increase VPD across the land surface[20], but these same models are much less certain about how soil moisture will be impacted by climate change[21,22]. These uncertainties impact evapotranspiration projections differently depending on how surface conductance is parameterized in climate models. Second, the relation among soil moisture, VPD and evapotranspiration is not necessarily stationary. Any relation may change as the climate warms and cause different environmental controls on evapotranspiration to become more or less dominant. The presence of non-stationary empirical relations has plagued studies of land-surface aridity; atmospheric proxies of land-surface aridity that work well in the present climate—such as simple aridity indices using potential evaporation—have been shown to offer unrealistic projections of warmer climate states[23–25]. Understanding the physical and biological drivers of surface conductance variability is required to move beyond empirical models of evapotranspiration to a physically consistent representation with appropriate causes and effects. Given the different uncertainties associated with soil moisture and VPD trends and the potential for underlying relations among land-surface properties to shift as the climate warms, illuminating the relation among soil moisture, VPD and ecosystem-scale surface conductance from available observations is an important task.

Here we hypothesize that observed relations between ecosystem-scale surface conductance and VPD that previous authors have attributed to stomatal regulation could, in fact, be driven by soil moisture rather than plant response to atmospheric humidity. Drier soils are known to reduce ecosystem-scale surface conductance in both vegetated[19] and non-vegetated ecosystems[26]. This results in lower evapotranspiration rates that drive higher atmospheric temperatures, higher VPD and lower relative humidity regardless of the underlying land cover. Given this, we expect lower surface conductance values in high-VPD environments and high surface conductance values in low-VPD environments independently of any stomatal regulation, due simply to the effect of water stress on evapotranspiration. If verified, our hypothesis suggests that the relation between surface conductance and VPD found in the observational literature can be at least partially explained by feedbacks among water limitation, ecosystem-scale surface conductance, evapotranspiration and boundary layer temperature.

Testing this hypothesis on an ecosystem scale is more difficult than it might first appear. Plant experiments—in laboratories or small plots—are not sufficient because they are not conducted at spatial scales sufficiently large to incorporate the land–atmosphere coupling that is crucial to our hypothesis. Instead, we must look for natural mechanism-denial experiments. An ideal site would have the following properties: (1) no vegetation, to eliminate any possibility of a stomatal response to VPD, and (2) an active hydrologic cycle, to make the analysis non-trivial. Such sites are rare in the real world because vegetation often grows rapidly following rainfall. We analyse three eddy covariance flux tower records from salt flats in Utah and Nevada (USA) that serve as laboratories for our mechanism-denial experiments. On these non-vegetated salt flats we find that the relation between surface conductance and VPD is similar to previously published relations that have been attributed to stomatal regulation by plants. This apparent contradiction illuminates not only the role of soil moisture in regulation of surface conductance over the salt flats, but how coupling between temperature and soil moisture can drive an emergent relation between VPD and surface conductance that can be misattributed to stomatal regulation. To complement our observational analysis we use an idealized boundary layer model to show how the relation between VPD and surface conductance found over the salt flats emerges naturally from coupling among soil moisture, evapotranspiration and near-surface air temperature. The emergent relation strongly resembles several empirical equations for stomatal conductance, even though we do not include any explicit representation of plant physiology in our model. Finally we illustrate how soil moisture measurement limitations, and the Penman–Monteith equation itself, may lead to the misattribution of variations in surface conductance to stomatal regulation driven by VPD fluctuations.

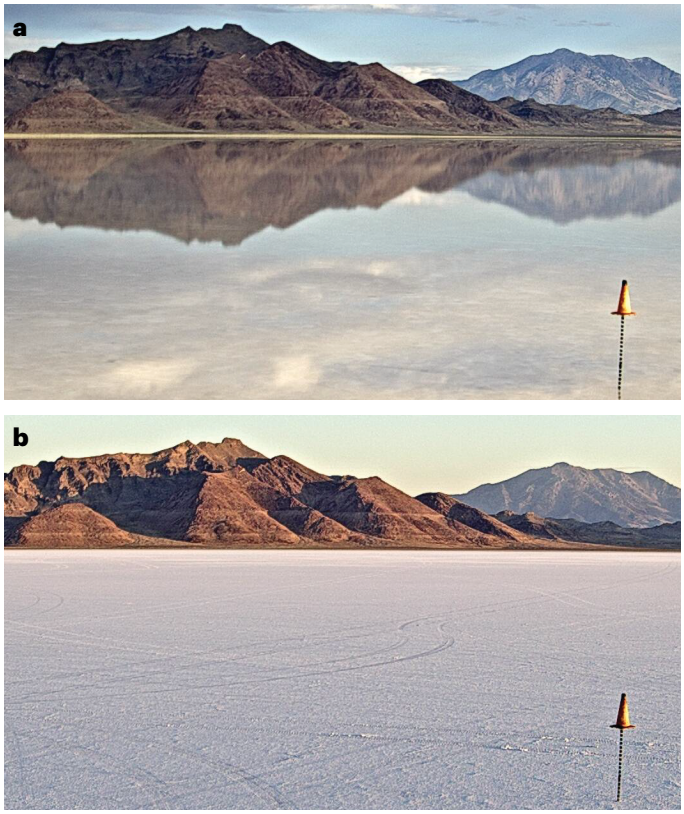

Fig. 1 | The Bonneville salt flats. a,**b**, Time-lapse photographs from the Bonneville salt flats on 28 May 2018, when the surface was flooded (**a**), and on 15 July 2018, when the surface was desiccated (**b**).

Surface conductance on the salt flats

Is surface conductance sensitive to VPD in an environment with no plants? To answer this question we analyse eddy covariance flux tower data from the Bonneville salt flats in Utah, and from two salt flats in Nevada's Dixie Valley (hereafter referred to as Playa 1 and Playa 2, respectively). These three ecosystems experience periods of flooding and desiccation but contain no vegetation. Figure 1 shows the hydrologic extremes exhibited by the Bonneville salt flats; for

https://doi.org/10.1038/s44221-023-00147-9

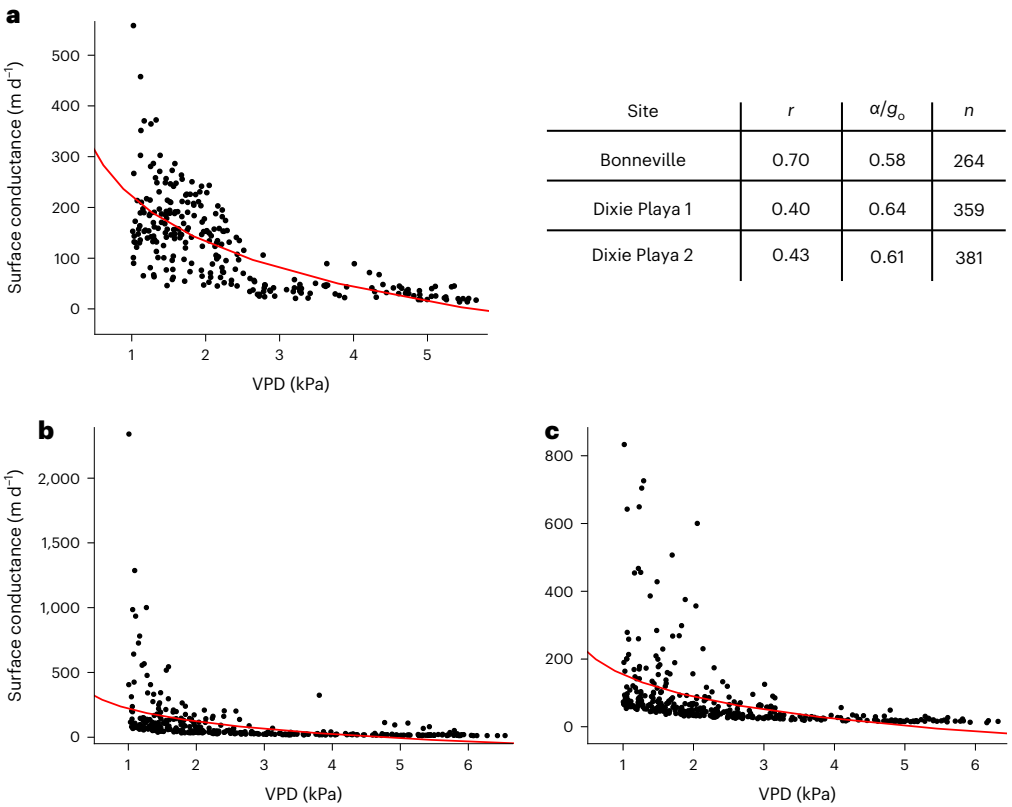

Site	r	α/g_o	n
Bonneville	0.70	0.58	264
Dixie Playa 1	0.40	0.64	359
Dixie Playa 2	0.43	0.61	381

Fig. 2 | Surface conductance on the salt flats. a–**c**, Surface conductance as a function of VPD over the three salt flat sites (Bonneville (**a**), Dixie Playa 1 (**b**) and Dixie Playa 2 (**c**)). The red line represents the best fit of the observations to the Oren model (equation (1)). Inset table shows the two-sided Pearson correlation coefficient r between estimated surface conductance from the various sites and the Oren model, the ratio α/g_o and the number of half-hourly observations that passed the data-screening procedure outlined in Methods.

similar photographs of all sites and details on data collection see Garcia et al.[27] and Bowen et al.[28].

For each of the three sites, Fig. 2 shows the surface conductance estimated by inversion of the Penman–Monteith equation as a function of VPD (see Methods for the relevant equations and data quality control details). The red line represents the best-fit curve to an empirical model for stomatal conductance (hereafter referred to as the Oren model[29]):

$$g_s = g_o - \alpha \ln(\mathrm{VPD}), \quad (1)$$

where g_s is surface conductance, α is a constant and g_o is a reference conductance value. In Oren et al.[29], the ratio α/g_o varies between 0.006 and 0.73 across various ecosystems, with 0.6 being the average value. The original study argued that this value was consistent with a simple hydraulic model of transpiration that included stomatal regulation, and is thus evidence for stomatal sensitivity to VPD on the ecosystem scale. Novick et al.[13] also used the Oren model to argue that stomatal regulation explains the observed relations between VPD and ecosystem-scale surface conductance. The table in Fig. 2 shows the correlation between data from the salt flats and the Oren model, along with the ratio α/g_o derived from the best fit of the salt flat data to equation (1). For all three sites the correlation with the Oren model is significant at the $P < 0.01$ level, and the α/g_o ratio is well within range of the values quoted above for the same ratio across vegetated ecosystems even though the mechanism behind this relation over the salt flats cannot be stomatal regulation. The correlations between surface conductance and ln(VPD) are comparable to (and in some cases much higher than) those found in other eddy covariance studies at vegetated sites[30,31]. To test the robustness of the results shown in Fig. 2 we also used a different method for estimation of surface conductance (inverting an equation for E that relies on surface temperature rather than 2 m air temperature). The results in Fig. 2 are not sensitive to the method used for estimation of surface conductance (Supplementary Fig. 1). We also note that our results are insensitive to how wet the soil surface is; Supplementary Fig. 2 shows surface conductance estimates composited by proximity to rainfall events in Playas 1 and 2—too few rainfall events occurred during the record encompassed in Fig. 2a to generate meaningful statistics.

Over the salt flats in Utah and Nevada we have found a nonlinear relation between observed VPD and surface conductance that appears very similar to an empirical model of stomatal conductance, both in terms of the empirically derived slope parameter (α/g_o) and the overall correlation between estimated surface conductance and ln(VPD). Previous authors have used this stomatal conductance model to argue that VPD controls surface conductance on an ecosystem scale[29], even when soil moisture variability is controlled for with a compositing analysis[13]. However, in ecosystems like the salt flats that have no stomata, the mechanism governing the relation between surface conductance and VPD must be the coupling of VPD and available soil moisture.

Surface conductance in an idealized boundary layer

Our observational analysis of surface conductance on the salt flats motivates a more general treatment of how coupling between soil moisture and temperature influences estimates of surface conductance. We consider a simple equilibrium model of land–atmosphere interaction based on McColl et al.[32] that, in turn, builds on previous studies[33–36]. The interested reader can find equations and parameter descriptions in Methods, but two important aspects of the model are

https://doi.org/10.1038/s44221-023-00147-9

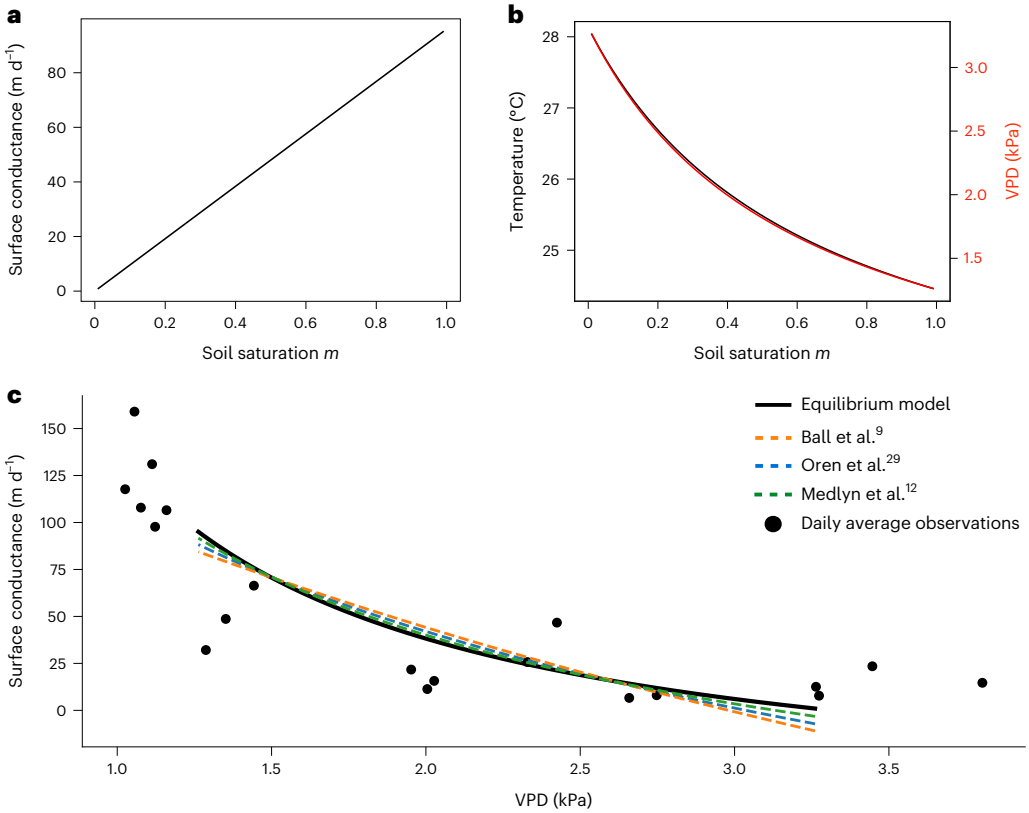

Fig. 3 | Surface conductance in the equilibrium model. a, The relation between surface conductance and soil moisture parameterized into the equilibrium model. **b**, The relations among atmospheric potential temperature, atmospheric VPD and soil moisture output from the equilibrium model. **c**, The emergent relation between surface conductance and VPD output by the boundary layer model. Also shown are VPD–conductance relations from three models of stomatal conductance and the daily-averaged observations of surface conductance and VPD from the Bonneville salt flats.

required to understand the results presented below. First, we apply a set of environmental forcings (net shortwave and downward longwave radiation, reference potential temperature and specific humidity, and soil moisture) to the model as a representation of diurnally averaged conditions. Second, we have not prescribed any relation between VPD and surface conductance in this model, only a linear dependence on soil moisture (Fig. 3a). This approach, implemented in the first numerical climate models, has been shown to reproduce key features of land-surface climatology[37].

Once the environmental forcings and model parameters have been specified, the model equations can be solved to determine the equilibrium potential temperature and VPD for different values of surface soil moisture (black and red lines in Fig. 3b). The equilibrium model output features a nonlinear relation between surface conductance and VPD that is driven entirely by the covariability of temperature and soil moisture shown in Fig. 3b. In Vargas Zeppetello et al.[38], a similar nonlinear relation between surface temperature and soil moisture was shown to be relatively insensitive to changes in surface parameters and environmental forcings. The exception is for extremely low values of maximum surface conductance that dampen the nonlinearity, but these correspond to trivial cases in which almost no evapotranspiration occurs. We tested the model sensitivity to parameter variations and found that our results were insensitive to realistic variations in the model parameters (Methods).

Because our model prescribes surface conductance purely as a function of soil moisture, we can use the VPD–soil moisture relation in Fig. 3b to construct the VPD–conductance relation that emerges purely due to coupling between soil moisture and boundary layer VPD (black line in Fig. 3c). We note that values of surface conductance output by our equilibrium model are lower than those from the half-hour averaged salt flat observations because we apply daily-averaged values for the downwelling radiation that are less noisy than the half-hour averaged data used to calculate g_s in Fig. 2. The diurnally averaged values for VPD and surface conductance from the Bonneville salt flats are also shown in Fig. 3c and are closer in magnitude to those from the boundary layer model. The same nonlinearity found over the salt flats is observed in the equilibrium model, and the physical mechanism in both cases is coupling between soil moisture and VPD via the influence of evaporation on the land surface and boundary layer energy budgets. In the experiments used to generate Fig. 3, the only physics captured by model is that soil moisture changes the evaporative fraction and, in turn, modifies boundary layer temperature, relative humidity and VPD.

The results shown in Fig. 3c are similar to several empirical models of stomatal regulation that have been used to argue that VPD controls ecosystem-scale surface conductance. Several models have been proposed to quantify the relation between VPD and stomatal (rather than surface) conductance; one empirical model is described above in equation (1)[29]. A multivariate analysis led to the development of the Ball–Berry equation[9], and another model was proposed by Medlyn et al.[12]. All three models feature VPD directly in the equations for stomatal conductance and are based on plant chamber experiments where soil water stress was not applied. While recent studies have investigated how model parameters associated with these models depend on soil moisture[13,39], the stomatal conductance models were originally designed to understand variations in leaf-level conductance and do not have a functional dependence on soil moisture. Therefore, they do not account for the relation between soil moisture and VPD that manifests on an ecosystem scale due to land–atmosphere coupling. Figure 3c

https://doi.org/10.1038/s44221-023-00147-9

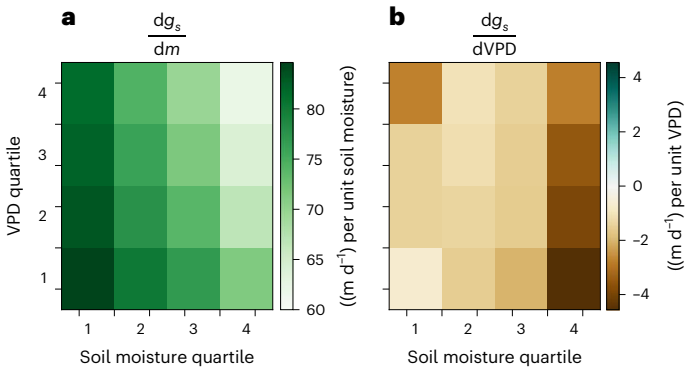

Fig. 4 | Surface conductance sensitivity to soil moisture and VPD. **a**,**b**, Estimated sensitivity of surface conductance to variations in soil moisture (**a**) and VPD (**b**) across soil moisture and VPD quartiles, using the inverted Penman–Monteith equation to estimate surface conductance with synthetic outputs from the equilibrium boundary layer model. All sensitivity values are calculated by a least-squares linear fit, and two-sided Pearson correlation coefficients between all variables are significant at the $P < 0.01$ level with Bonferroni correction appropriate for a family of 16 hypotheses.

shows the stomatal conductance values obtained from substitution of the VPD and potential temperature values given by our equilibrium model into the Ball–Berry equation, the empirical Oren model and the Medlyn equation. All parameters in these models were tuned to give the best fit to the black curve in Fig. 3c (Methods).

The correlation between the Medlyn model (green line in Fig. 3c) and the relation obtained from the equilibrium model (black line in Fig. 3c) is 0.99. The same correlation is found for the Oren et al. empirical model[29] (blue line in Fig. 3c). For the Ball–Berry model (orange line in Fig. 3c) the correlation is 0.98. To determine the robustness of our results we tested the various combinations of model parameters and environmental forcings detailed in Supplementary Table 1. These variations slightly alter the shape of the VPD–surface conductance relation shown in Fig. 3c, but all parameter variations result in curves that are highly correlated with the Oren model ($r > 0.95$ for all parameter choices with $P < 0.01$). Varying environmental forcings led to values of α/g_o between 0.47 and 0.80, while variations in the surface parameters applied to the model led to values of α/g_o between 0.60 and 1.11. The spread in these values across a variety of surface parameterizations and background climate states is comparable to the spread found in Oren et al.[29] and more recent work that used the same model to determine these relations across different ecosystems[13]. Differences in background climate and surface parameters have the potential to explain the spread in α/g_o previously attributed to differences in stomatal control on transpiration across species. While it could be argued that the results presented in Fig. 3 depend on a linear parameterization of E as a function of soil moisture, we tested the model with several different parameterizations of surface conductance as a function of soil moisture and found that the high correlations with the Ball–Berry, Medlyn and Oren models hold in general for any parameterization of ecosystem-scale surface conductance as an increasing functions of soil moisture.

Variations in the slope of the VPD–conductance relationship have been shown to vary with background soil moisture. Both Novick et al.[13] and Fu et al.[17] used a compositing analysis to isolate the influence of VPD on surface conductance within particular soil moisture bins. However, the black curve in Fig. 3c suggests that the slope of the VPD–conductance relation should depend on climatological VPD and that, in particular, we should expect larger magnitude slopes in low-VPD bins (where the derivative of the curve shown in Fig. 3c is largest) that also correspond to the highest soil moisture values. While Fu et al.[17] and Novick et al.[13] have argued that the sensitivity of the VPD–g_s curve to background state is evidence for stomatal control on ecosystem-scale surface conductance, the simple model reproduces key findings from these studies without any parameterization of stomatal regulation. We used one million sets of random forcings (Methods and Supplementary Table 2) to calculate surface conductance and VPD from our equilibrium model and then binned results into VPD and soil moisture quartiles. For each combination of VPD and soil moisture quartile, Fig. 4 shows the sensitivity of surface conductance to changes in soil moisture $\frac{dg_s}{dm}$ and VPD $\frac{dg_s}{dVPD}$.

The sensitivity analysis from the stomata-free boundary layer model shown in Fig. 4 qualitatively agrees with the findings of earlier studies that attributed variations across soil moisture and VPD quantiles to stomatal regulation. Novick et al.[13] also showed increasing values of the VPD–g_s slope as a function of soil moisture within VPD bins, which is also shown in Fig. 4 for all but the driest soil moisture quartile where average surface conductance is extremely low. Without invoking stomatal closure, we find reduced sensitivity of surface conductance to soil moisture in higher-soil-moisture quartiles and increased sensitivity of surface conductance to VPD at lower-VPD and higher-soil-moisture quartiles. Both of these results can be found in figure 2b,e of Fu et al.[17], although those authors divided their soil moisture and VPD data into ten bins each (see Supplementary Information for a discussion of these results). In summary, the sensitivity of the VPD–g_s curve to the underlying soil moisture values can be explained by the nonlinear relation between VPD and surface conductance found in Fig. 3c and does not depend on stomatal closure.

In our equilibrium model, coupling between soil moisture and VPD is sufficient to explain variations in surface conductance that have been attributed to stomatal regulation in response to VPD fluctuations. On an ecosystem scale, the boundary layer model exhibits the same relation between VPD and surface conductance attributed by previous studies to stomatal regulation even though it contains no explicit representation of plant activity. In our equilibrium boundary layer model, a drier land surface has lower ecosystem-scale surface conductance and drives atmospheric drying (higher VPD), rather than vice versa. The similarity of results from our model to established stomatal conductance equations (Fig. 3c) suggests that the relation between soil moisture and VPD, produced by the sensitivity of the boundary layer to land-surface energy partitioning, could easily be misattributed to stomatal regulation in response to VPD fluctuations if stomatal conductance equations, such as the Ball–Berry model, are uncritically applied to data collected at the ecosystem scale.

Measurement errors

The results from the salt flats and the equilibrium boundary layer model suggest that land–atmosphere coupling explains the relation between VPD and surface conductance that previous authors have attributed to stomatal closure. Past studies have attempted to control for land–atmosphere coupling in various ways, including compositing data to examine surface conductance variability within a fixed soil moisture range[13,17] and developing statistical models that link VPD, surface conductance and soil moisture[14,16,40]. Despite the known link between soil moisture and surface conductance, VPD has consistently been shown to explain more variance in estimated surface conductance than soil moisture, bolstering the hypothesis that stomatal regulation in response to humidity fluctuations drives surface conductance variability.

We hypothesize that one reason for the disagreement between previous studies and our results is that soil moisture observations, but not VPD observations, are subject to considerable 'representativeness errors' that are not acknowledged in the observational studies cited above. For our purposes, representativeness errors concern point-scale measurements taken at eddy covariance flux towers that do not reflect the mean conditions over the spatial footprint required for ecosystem-scale analysis. For VPD this is not a concern because the atmosphere's turbulent mixing in the boundary layer makes point-scale measurements sufficient for determination of the ecosystem-scale average. In contrast, any single point-scale soil moisture observation is a relatively imprecise estimate of the large-scale average value due to the land

surface's spatial (and vertical) heterogeneity[41,42]. We refer to the differences between point-scale measurements and the mean of the spatial field they seek to represent as representativeness errors in point-scale measurements. These are distinct from other measurement errors and result purely from estimation of the mean of a heterogeneous field from a single sample[43]. We hypothesize that these errors, combined with the physical mechanism articulated above, may cause VPD to appear more correlated with surface conductance than observed soil moisture, even when soil moisture drives surface conductance variability.

Given the physical mechanism linking soil moisture and surface conductance, the presence of substantial representativeness errors in soil moisture, but not in VPD, is sufficient to cause VPD to appear more correlated with surface conductance than soil moisture in observational analyses. To illustrate this we performed two experiments by forcing the equilibrium boundary layer model with random variations in all environmental forcings (net radiation, reference potential temperature and reference specific humidity) and soil moisture. Details on these randomized forcings are found in Methods. For each realization of the equilibrium model we calculated atmospheric VPD and used an inversion of the Penman–Monteith equation to estimate surface conductance. In each experiment we used 10,000 randomly sampled combinations of environmental forcings and soil moisture values.

Results from the first experiment ('control') are shown in Fig. 5a,b, where estimated surface conductance from each model realization is plotted as a function of soil moisture and VPD, respectively. In the control experiment, surface conductance and soil moisture are almost perfectly correlated; this is not surprising, because surface conductance in the boundary layer model is given as a linear function of soil moisture (Methods) as opposed to some other nonlinear function[44]. As discussed above, this relation between surface conductance and soil moisture is reflected in the conductance–VPD relation where the same behaviour shown in Fig. 3c is found, along with a significant ($P < 0.01$) correlation with the best fit of the derived surface conductance to equation (1). Correlation values between VPD and surface conductance found in the control experiment are similar to other observational estimates[30,31].

The second experiment ('Soil moisture errors' in Fig. 5) is identical to the control experiment, except that synthetic representativeness errors (here represented by white noise) are added to the soil moisture values plotted in Fig. 5c following the completion of simulations. The s.d. of white noise is tuned such that the correlation between the original soil moisture applied to the model and the 'noise added' soil moisture plotted in Fig. 5c is the same as we would expect for two soil moisture probes placed 1 m apart in the soil column ($r^2 = 0.14$)[45]. After the addition of noise we restrict the range of soil moisture values to between zero and one. Figure 5c,d shows results from a hypothetical experiment where (1) plants have no role in surface conductance and (2) realistic representativeness errors are present in soil moisture observations but not in VPD observations. In this case the correlation between soil moisture and derived surface conductance drops substantially compared with the control experiment, while the correlation between VPD and the Oren model of stomatal conductance is unchanged. Focusing on correlation coefficients would lead to the incorrect conclusion that fluctuations in VPD explain more variability in surface conductance than fluctuations in soil moisture, even though this is definitively not the case in our synthetic experiment.

Previous studies do not account for the fact that representativeness errors are much greater in observations of soil moisture than in those of VPD. For example, Flo et al.[16] used multiple linear regression models that included different combinations of soil moisture and VPD and compared r^2 values of models that included one variable or the other. They found higher fractions of explained variance in models that included VPD relative to those that included only soil moisture. This is not surprising given that our result in Fig. 5 shows the degree to which the explanatory power of soil moisture can deteriorate because of underlying representativeness errors. Representativeness errors may also reduce the efficacy of analyses that condition on specific soil moisture ranges[13,17]. The degree to which this problem impacts the neural network methodology deployed in Fu et al.[17], the path analysis of Kimm et al.[14] or the compositing analyses of Novick et al.[13] is less clear. However, since none of those approaches explicitly addresses the problem of differences in measurement errors between soil moisture and VPD, there is no reason to expect they would be any less confounded. In general, any observational data analysis (including nonlinear approaches that employ machine learning) will still remain sensitive to fundamental differences in measurement errors between VPD and soil moisture.

Equation bias

Even if the representativeness errors discussed above were to be overcome, the structure of equations used to determine surface conductance from observations virtually ensures that relations will be found between VPD and surface conductance that resemble empirical models of stomatal conductance. Figure 6 shows surface conductance as a function of VPD using uncorrelated Gaussian noise for the inputs into two different inversion equations for surface conductance (Methods). In both cases the scatter is significantly correlated ($P < 0.01$) with the Oren model of stomatal conductance. In addition, the application of Gaussian noise to both equations generates α/g_o ratios within the range across ecosystems given by Oren et al.[29]. Random variations are apparently more than adequate to generate the observed relation between surface conductance and VPD—even without the mechanism of land–atmosphere coupling discussed above.

The reason that random variability input into both equations for estimation of surface conductance (equations (3) and (6); Methods) generates VPD–g_s relations similar to those found in observations is that measures of atmospheric humidity appear directly in these equations. In both methods for estimation of surface conductance that we have discussed (both of which are widely used in other studies), surface conductance depends directly on atmospheric humidity but not on soil moisture. Based on the results shown in Fig. 6, it is unsurprising that VPD has been found to be the dominant driver of surface conductance variability rather than soil moisture, a variable that does not appear directly in surface conductance equations. The fact that random numbers input into equations for estimation of surface conductance generate relations that appear similar to established models of stomatal regulation indicates that extreme care must be taken when applying these models to the ecosystem scale. In general, any analysis that uses the Penman–Monteith equation to estimate surface conductance will impose structure on the VPD–surface conductance relation that appears similar to structure attributed to stomatal regulation, even when stomatal regulation does not contribute to variations in surface conductance.

Conclusions

In the natural laboratory of the non-vegetated salt flats, and our idealized boundary layer model that contains no representation of stomatal regulation, we have found that the apparent surface conductance sensitivity to VPD is driven by variations in soil moisture. Our study is limited by the small number of non-vegetated, hydrologically active ecosystems where flux tower data are collected, but our results are similar across the three sites we analysed. The boundary layer model is highly idealized and includes no representation of thermal advection. However, the effect of advection on the near-surface atmospheric state in continental regions is typically secondary to that of local surface fluxes[36,46,47]. The findings from the boundary layer model are therefore generalizable, even in vegetated regions. Our results do not negate the possibility of stomatal regulation influencing surface conductance variability. They do suggest, however, that uncritical application of stomatal conductance models to explain surface conductance variability at ecosystem scales can lead to misattribution of the observed variability to VPD fluctuations when the underlying mechanism may be soil moisture variability. Importantly, this result complicates previous

https://doi.org/10.1038/s44221-023-00147-9

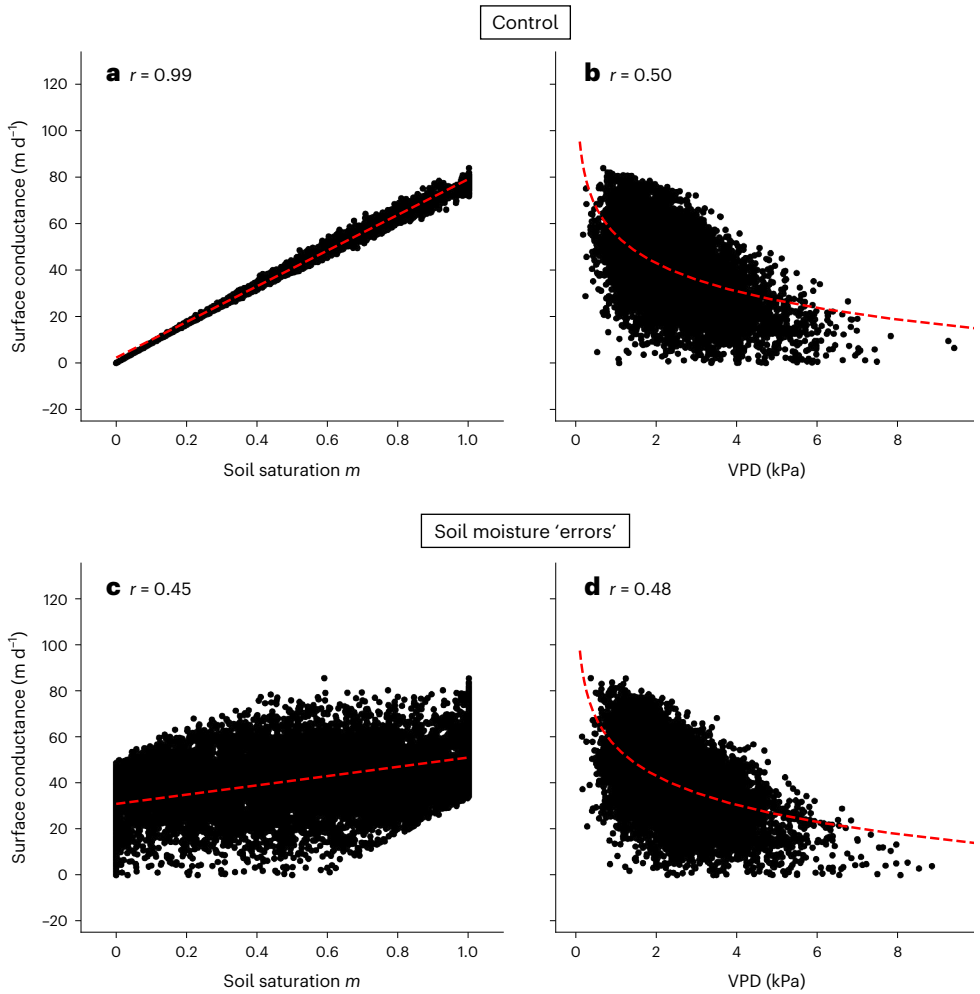

Fig. 5 | Synthetic measurement errors. a–**d**, Surface conductance as a function of soil moisture (**a**,**c**) and VPD (**b**,**d**) from two experiments with our equilibrium model. In the first we forced the model with random noise (Methods) and derived surface conductance by inversion of the Penman–Monteith equation (**a**,**b**). In the second we did the same but also added random noise to the soil moisture time series following completion of the simulation, to emulate representativeness errors in soil moisture (**c**,**d**). Red dashed lines represent the best-fit linear regression (**a**,**c**) and the best fit to the Oren model (**b**,**d**).

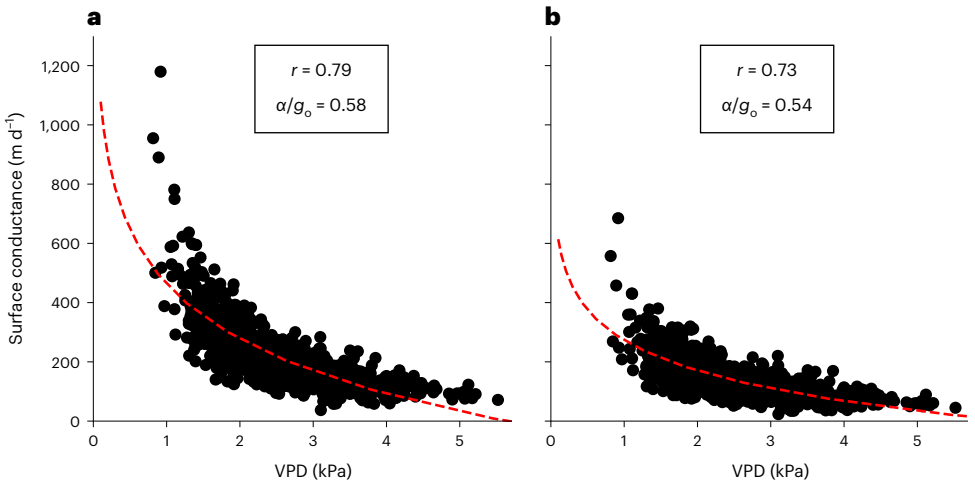

Fig. 6 | Surface conductance equation bias. a,**b**, Surface conductance as a function of VPD using random inputs into two equations for surface conductance. **a**, Results for a direct inversion that requires surface temperature as an input. **b**, Results from an inversion of the Penman–Monteith equation (Methods). Red dashed lines represent the best fit of relations to the Oren model. Two-sided Pearson correlation *r* measures the fit of randomly generated surface conductance values to the Oren model. See discussion of equation (1) for definitions of α and g_o. **a**,**b**, 1,000 sets of random inputs.

findings that increases in VPD driven by anthropogenic climate change will drive decreases in surface conductance and, by extension, evapotranspiration. Instead, our results suggest that soil moisture, and not VPD, is the relevant state variable for understanding how surface conductance will evolve in a warmer world. Because soil moisture projections are highly uncertain[22], we remain agnostic on making projections of future changes in surface conductance in this study.

Two problems, one technological and one theoretical, prevent us (or any study) from making more definitive statements about the dominant environmental controls on ecosystem-scale surface conductance. The first problem concerns representativeness errors: capturing the soil moisture variability relevant to ecosystem-scale surface conductance (or evapotranspiration) with contemporary point-scale or satellite measurements of soil moisture is very difficult. For any study of ecosystem-scale surface conductance to be definitive, a truly representative soil moisture value must be defined and measured. It might seem that the difference in representativeness errors between VPD and soil moisture could be corrected by normalizing both quantities by their respective observed temporal variances[48]. This correction assumes that temporal variance is a reasonable estimate of spatial variance, but this assumption is very strongly violated for soil moisture[49]. Representativeness errors also present a problem in regard to ecosystems with deep roots, because the available point measurements may not be appropriate for rooting depth profiles that, in general, are highly nonlinear[50]. While we have argued from a physical perspective that land–atmosphere coupling is sufficient to describe the observed relation between VPD and surface conductance, we have not conclusively shown that soil moisture is having a dominant role in evapotranspiration. In fact, given the representativeness errors in soil moisture observations, such a goal is very difficult to achieve with existing technology.

The theoretical problem concerns biases in the equations used to determine surface conductance that typically contain atmospheric variables (such as air temperature and humidity) but not land-surface variables (such as soil moisture). Without more comprehensive theories of evapotranspiration that explicitly account for soil moisture variability, important questions about the role of plant–atmosphere coupling in governing surface conductance will be biased in favour of easily measurable atmospheric-state variables. Although this does not mean that plants cannot influence surface conductance on an ecosystem scale, it does mean that surface conductance estimates generated by established equations that do not include soil moisture state require careful analysis to isolate the true role of plant physiology on photosynthesis (not unlike other emergent ecosystem properties discussed in Lloyd et al.[51]). In particular, analyses that include both water and carbon fluxes may be an avenue towards improving our understanding of variations in surface conductance. We have shown that land–atmosphere coupling is sufficient to explain the observed relation between VPD and surface conductance on an ecosystem scale; further work is needed to determine the exact role that plant physiology has in the regulation of continental evapotranspiration.

Methods

Two methods for estimation of surface conductance

The Penman–Monteith approach is useful for determination of equilibrium evapotranspiration and surface conductance if no data for surface temperature exist. Rather than information on surface temperature, 2 m air temperature T_a is an input to the Penman–Monteith equation:

$$\lambda \times E = \frac{\Delta(R_n - G) + c_a\rho_a g_a(q_s(T_a) - q)}{\Delta + \gamma\left(1 + \frac{g_a}{g_s}\right)}, \quad (2)$$

where q_s and q are saturation and 2 m specific humidity, respectively, Δ is $\frac{de_s}{dT}$ evaluated at air temperature T_a, R_n is net radiation, G is ground heat flux, c_a the specific heat of dry air and $\gamma = c_a/\lambda$. Solving for g_s, we obtain

$$g_s = g_a\gamma\left(\frac{\Delta(R_n - G) + c_a\rho_a g_a(q_s(T_a) - q)}{\lambda \times E} - \Delta - \gamma\right)^{-1}. \quad (3)$$

Aerodynamic conductance is given by

$$g_a = \frac{uk^2}{\ln\left(\frac{z_m - z_d}{z_o} - \Phi_M\right)\ln\left(\frac{z_m - z_d}{z_o} - \Phi_H\right)}, \quad (4)$$

where u is wind speed, k is the von Kármán constant, z_m is measurement height (2 m in our case), z_d is zero plane displacement height and z_o is momentum roughness length[4]. These last two length scales are functions of canopy height h ($z_o = 0.1h$ and $z_d = 0.67h$). We set $h = 0.1$ m, in line with previous studies of desert environments[52]. The terms Φ_H and Φ_M are stability corrections to equation (4) as detailed as Paulson[53] and Holstag and DeBruin[54].

Following Novick et al.[13], we screened out flux tower data taken when net radiation was <50 W m^{-2} and when latent heat flux was <20 W m^{-2}. These thresholds ensured that only daylight periods where latent heat flux made up a substantial fraction of the surface energy balance were included in the analysis. We also screened out measurements taken when wind speed was <1 m s^{-1}, and those taken when VPD was <1 kPa, to minimize stability effects. In addition, the Nevada sites had a substantial amount of measurements where the surface energy budget was not balanced. We screened out measurements where the absolute value of the imbalance (given by $R_n - H - G - L \times E$) was 10% of total net radiation (H is surface sensible heat flux). The Bonneville salt flats have a record of net radiation and latent heat flux; because no data on ground heat flux were taken, we assumed this flux to be zero.

The Penman–Monteith equation is based on the following equation for E that is a function of evaporating surface temperature T_s (refs. 2,3):

$$E = \frac{\rho_a g_s g_a}{g_a + g_s}(q_s(T_s) - q). \quad (5)$$

The second method for estimation of surface conductance, used to construct Supplementary Fig. 1, is based on rearranging the terms in equation (5) and gives surface conductance as

$$g_s = g_a\left(\frac{g_a\rho_a(q_s(T_s) - q)}{E} - 1\right)^{-1}. \quad (6)$$

In the Bonneville data, evaporation rate E is observed directly in kg H_2O m^{-2} s^{-1}. The Bonneville flux tower data include outgoing longwave radiation from the land surface. By assuming a longwave emissivity of 1, we inverted the Stefan–Boltzmann law to determine local surface temperature T_s then calculated saturation-specific humidity at this value (and surface pressure) to obtain $q_s(T_s)$.

Boundary layer model description

For an idealized zero-heat capacity land surface in equilibrium, land-surface energy balance is

$$0 = R_n - \lambda E - H, \quad (7)$$

where net radiation $R_n = S_n + L_\downarrow - \sigma T_s^4$ is a balance between net downward shortwave radiation S_n, downward longwave radiation $L_\downarrow$ and upward longwave radiation that depends on surface temperature T_s (we assume that the surface radiates like a perfect black body); λ is the latent enthalpy of vaporization for water and H is surface sensible heat

flux. To incorporate soil moisture into the equation for E, we modify equation (5) such that surface conductance increases linearly with soil moisture:

$$E = \frac{\rho_a g_o m g_a}{g_a + g_o m}(q_s(T_s) - q), \tag{8}$$

where g_o is maximum surface conductance and m is soil saturation, a value between 0 and 1, with 0 corresponding to the wilting point and 1 corresponding to field capacity.

Sensible heat flux H is given by

$$H = \rho_a c_a g_a (T_s - \theta), \tag{9}$$

where c_a is the specific heat of dry air and θ is the potential temperature of the atmospheric boundary layer.

In equilibrium, the energy balance in the atmospheric boundary layer is

$$0 = H + \frac{\rho_a c_a h_a}{\tau_R}(\theta_R - \theta), \tag{10}$$

Boundary layer height, h_a, is treated as a fixed parameter, consistent with previous models of the diurnally averaged boundary layer[32–36,55,56]. The τ_R value determines how quickly boundary layer potential temperature relaxes towards some free tropospheric reference value θ_R; the second term in equation (10) is a simple parameterization of processes that cool the boundary layer, such as radiative cooling and thermal advection.

The equilibrium moisture budget in the atmospheric boundary layer is

$$0 = E + \frac{\rho_a h_a}{\tau_R}(q_R - q), \tag{11}$$

where q_R is the reference specific humidity towards which q evolves in the absence of evapotranspiration; the second term in equation (11) is a simple parameterization of processes that dry the boundary layer, such as dry-air entrainment and cloud-base mass flux. The boundary layer model requires specification of soil moisture m, four model parameters (g_o, g_a, h_a and τ_R) and four environmental forcings (S_n, $L_\downarrow$, θ_R and q_R) to solve for T_s, θ and q. Supplementary Table 1 shows the parameters and environmental forcings applied to the equilibrium model to generate Fig. 3, along with values used in sensitivity tests in parenthesis.

Stomatal conductance equations

The Ball–Berry model gives stomatal conductance as

$$g_s = \frac{\beta A}{c_s}\left(1 - \frac{\mathrm{VPD}}{e_s(\theta)}\right) + \Gamma, \tag{12}$$

where A is photosynthetic rate, c_s is CO_2 concentration at the leaf surface, Γ is a reference conductance parameter and β is a constant[9]. The Medlyn model gives stomatal conductance as

$$g_s = \frac{1.6 \times A}{c_s}\left(1 + \frac{g_1}{\sqrt{\mathrm{VPD}}}\right), \tag{13}$$

where g_1 is a parameter derived from a theory of optimal stomatal behaviour[12]. Note that values of stomatal conductance can be given with two different sets of units: velocity (m s^{-1}) or molar flux per unit area (mmol m^{-2} s^{-1}). We use the former, which is consistent with the formulation of equation (5); the latter is more common in plant physiological literature. A linear scaling involving the molar mass and density of water can be used to convert between the two sets of units.

Stochastic inputs to the boundary layer model

The model parameters shown in Supplementary Table 1 were used to generate the plots in Figs. 4 and 5. However, environmental forcings were drawn from Gaussian distributions with specified mean μ_X and s.d. σ_X for each distribution. These values are listed in Supplementary Table 2. Importantly, we have not included correlations between environmental forcings; we performed an additional set of experiments where variations in net radiation, reference potential temperature and reference specific humidity were correlated with one another (by drawing all random values from the same distribution and then scaling them appropriately), and found that the major results were insensitive to correlations between samples. Therefore, we expect the correlated nature of environmental forcings to be a second-order effect that does not impact the results discussed in Figs. 4 and 5.

To generate Fig. 6, random numbers were drawn from a separate Gaussian distributions—again we have not included any covariance among our input variables. Supplementary Table 3 shows the inputs to equations (3) and (6), and Fig. 6 shows surface conductance values obtained through this exercise.

Reporting summary

Further information on research design is available in the Nature Portfolio Reporting Summary linked to this article.

Data availability

The Bonneville dataset analysed in the current study is available at https://github.com/Lvargaszeppetello/Surface_Conductance. The Dixie Valley salt flat data are available online at https://waterdata.usgs.gov/monitoring-location/394508118025505/#parameterCode=62968&startDT=2009-05-01&endDT=2010-05-01 and https://waterdata.usgs.gov/monitoring-location/394559118013705/#parameterCode=62968&startDT=2009-05-01&endDT=2010-05-01.

Code availability

All analysis code is available at https://github.com/Lvargaszeppetello/Surface_Conductance.

References

1. Stephens, G. L. et al. An update on earth's energy balance in light of the latest global observations. *Nat. Geosci.* **5**, 691–696 (2012).
2. Penman, H. Natural evaporation from open water, bare soil and grass. *Proc. R. Soc. Lond. A Math. Phys. Sci.* **193**, 120–145 (1948).
3. Monteith, J. Evaporation and surface temperature. *Q. J. R. Meteorol. Soc.* **107**, 1–27 (1981).
4. Campbell, G. S. & Norman, J. M. *An Introduction to Environmental Biophysics* (Springer Science & Business Media, 2000).
5. Penman, H. The dependence of transpiration on weather and soil conditions. *J. Soil Sci.* **1**, 74–89 (1950).
6. Thom, A. & Oliver, H. R. On Penman's equation for estimating regional evaporation. *Q. J. R. Meteorol. Soc.* **103**, 345–357 (1977).
7. Darwin, F. Ix. Observations on stomata. *Philos. Trans. R. Soc. Lond. B Biol. Sci.* **63**, 589–600 (1898).
8. Lange, O. L., Lösch, R., Schulze, E. D. & Kappen, L. Responses of stomata to changes in humidity. *Planta* **100**, 76–86 (1971).
9. Ball, J. T., Woodrow, I. E. & Berry, J. A. in *Progress in Photosynthesis Research* (ed. Biggins, J.) 221–224 (Springer, 1987).
10. Turner, N. C., Schulze, E.-D. & Gollan, T. The responses of stomata and leaf gas exchange to vapour pressure deficits and soil water content: I. Species comparisons at high soil water contents. *Oecologia* **63**, 338–342 (1984).
11. Franks, P., Cowan, I. & Farquhar, G. The apparent feedforward response of stomata to air vapour pressure deficit: information revealed by different experimental procedures with two rainforest trees. *Plant Cell Environ.* **20**, 142–145 (1997).

12. Medlyn, B. E. et al. Reconciling the optimal and empirical approaches to modelling stomatal conductance. *Glob. Chang. Biol.* **17**, 2134–2144 (2011).
13. Novick, K. et al. The increasing importance of atmospheric demand for ecosystem water and carbon fluxes. *Nat. Clim. Change* **6**, 1023–1027 (2016).
14. Kimm, H. et al. Redefining droughts for the U.S. corn belt: the dominant role of atmospheric vapor pressure deficit over soil moisture in regulating stomatal behavior of maize and soybean. *Agric. For. Meteorol.* **287**, 107930 (2020).
15. Roby, M. C., Scott, R. L. & Moore, D. J. High vapor pressure deficit decreases the productivity and water use efficiency of rain-induced pulses in semiarid ecosystems. *J. Geophys. Res. Biogeosci.* **125**, e2020JG005665 (2020).
16. Flo, V., Martínez-Vilalta, J., Granda, V., Mencuccini, M. & Poyatos, R. Vapor pressure deficit is the main driver of tree canopy conductance across biomes. *Agric. For. Meteorol.* **322**, 109029 (2022).
17. Fu, Z. et al. Atmospheric dryness reduces photosynthesis along a large range of soil water deficits. *Nat. Commun.* **13**, 989 (2022).
18. Mott, K. A. & Parkhurst, D. F. Stomatal responses to humidity in air and helox. *Plant Cell Environ.* **14**, 509–515 (1991).
19. Buckley, T. N. How do stomata respond to water status? *New Phytol.* **224**, 21–36 (2019).
20. Grossiord, C. et al. Plant responses to rising vapor pressure deficit. *New Phytol.* **226**, 1550–1566 (2020).
21. Berg, A., Sheffield, J. & Milly, P. C. Divergent surface and total soil moisture projections under global warming. *Geophys. Res. Lett.* **44**, 236–244 (2017).
22. Cook, B. I. et al. Twenty-first century drought projections in the CMIP6 forcing scenarios. *Earths Future* **8**, e2019EF001461 (2020).
23. Roderick, M. L., Greve, P. & Farquhar, G. D. On the assessment of aridity with changes in atmospheric CO_2. *Water Resour. Res.* **51**, 5450–5463 (2015).
24. Swann, A. L., Hoffman, F. M., Koven, C. D. & Randerson, J. T. Plant responses to increasing CO_2 reduce estimates of climate impacts on drought severity. *Proc. Natl Acad. Sci. USA* **113**, 10019–10024 (2016).
25. Berg, A. & McColl, K. No projected global drylands expansion under greenhouse warming. *Nat. Clim. Change* **11**, 331–337 (2021).
26. Wythers, K., Lauenroth, W. & Paruelo, J. Bare-soil evaporation under semiarid field conditions. *Soil Sci. Soc. Am. J.* **63**, 1341–1349 (1999).
27. Garcia, C. A. et al. *Groundwater discharge by evapotranspiration, Dixie Valley, Westcentral Nevada, March 2009–September 2011*. US Geological Survey Professional Paper (USGS, 2015); https://doi.org/10.3133/pp1805
28. Bowen, B. B., Kipnis, E. L. & Raming, L. W. Temporal dynamics of flooding, evaporation, and desiccation cycles and observations of salt crust area change at the Bonneville salt flats, Utah. *Geomorphology* **299**, 1–11 (2017).
29. Oren, R. et al. Survery and synthesis of intra- and interspecific variation in stomatal sensitivity to vapour pressure deficit. *Plant Cell Environ.* **22**, 1515–1526 (1999).
30. Lin, C. et al. Diel ecosystem conductance response to vapor pressure deficit is suboptimal and independent of soil moisture. *Agric. For. Meteorol.* **250–251**, 24–34 (2018).
31. Kannenberg, S. A. et al. Quantifying the drivers of ecosystem fluxes and water potential across the soil-plant-atmosphere continuum in an arid woodland. *Agric. For. Meteorol.* **329**, 109269 (2022).
32. McColl, K. A., Salvucci, G. D. & Gentine, P. Surface flux equilibrium theory explains an empirical estimate of water-limited daily evapotranspiration. *J. Adv. Model. Earth Syst.* **11**, 2036–2049 (2019).
33. Brubaker, K. L. & Entekhabi, D. An analytic approach to modeling land-atmosphere interaction: 1. Construct and equilibrium behavior. *Water Resour. Res.* **31**, 619–632 (1995).
34. Kim, C. & Entekhabi, D. Feedbacks in the land-surface and mixed-layer energy budgets. *Boundary Layer Meteorol.* **88**, 1–21 (1998).
35. Raupach, M. R. Equilibrium evaporation and the convective boundary layer. *Boundary Layer Meteorol.* **96**, 107–142 (2000).
36. Betts, A. K. Idealized model for equilibrium boundary layer over land. *J. Hydrometeorol.* **1**, 507–523 (2000).
37. Manabe, S. Climate and the ocean circulation: I. The atmospheric circulation and the hydrology of the earth's surface. *Mon. Weather Rev.* **97**, 739–774 (1969).
38. Vargas Zeppetello, L., Battisti, D. & Baker, M. The physics of heat waves: what causes extremely high summertime temperatures? *J. Clim.* **35**, 2231–2251 (2022).
39. Tarin, T., Nolan, R. H., Medlyn, B. E., Cleverly, J. & Eamus, D. Water-use efficiency in a semi-arid woodland with high rainfall variability. *Glob. Chang. Biol.* **26**, 496–508 (2020).
40. Sulman, B. N. et al. High atmospheric demand for water can limit forest carbon uptake and transpiration as severely as dry soil. *Geophys. Res. Lett.* **43**, 9686–9695 (2016).
41. Western, A. W., Grayson, R. B. & Blöschl, G. Scaling of soil moisture: a hydrologic perspective. *Annu. Rev. Earth Planet. Sci.* **30**, 149–180 (2002).
42. Famiglietti, J. S., Ryu, D., Berg, A. A., Rodell, M. & Jackson, T. J. Field observations of soil moisture variability across scales. *Water Resour. Res.* **44**, W01423 (2008).
43. Gruber, A. et al. Recent advances in (soil moisture) triple collocation analysis. *Int. J. Appl. Earth Obs. Geoinf.* **45, Part B**, 200–211 (2016).
44. Trugman, A. T., Medvigy, D., Mankin, J. & Anderegg, W. R. Soil moisture stress as a major driver of carbon cycle uncertainty. *Geophys. Res. Lett.* **45**, 6495–6503 (2018).
45. Feldman, A. F. et al. Remotely sensed soil moisture can capture dynamics relevant to plant water uptake. *Water Resour. Res.* **59**, e2022WR033814 (2023).
46. McColl, K. A. Practical and theoretical benefits of an alternative to the penman-monteith evapotranspiration equation. *Water Resour. Res.* **56**, e2020WR027106 (2020).
47. Chen, S., McColl, K. A., Berg, A. & Huang, Y. Surface flux equilibrium estimates of evapotranspiration at large spatial scales. *J. Hydrometeorol.* **22**, 765–779 (2021).
48. Koster, R. D. et al. On the nature of soil moisture in land surface models. *J. Clim.* **22**, 4322–4335 (2009).
49. Teuling, A. J., Uijlenhoet, R., Hupet, F., van Loon, E. E. & Troch, P. A. Estimating spatial mean root-zone soil moisture from point-scale observations. *Hydrol. Earth Syst. Sci.* **10**, 755–767 (2006).
50. Jackson, R. B. et al. A global analysis of root distributions for terrestrial biomes. *Oecologia* **108**, 389–411 (1996).
51. Lloyd, J., Bloomfield, K., Domingues, T. F. & Farquhar, G. D. Photosynthetically relevant foliar traits correlating better on a mass vs an area basis: of ecophysiological relevance or just a case of mathematical imperatives and statistical quicksand? *New Phytol.* **199**, 311–321 (2013).
52. Raupach, M. Vegetation-atmosphere interaction and surface conductance at leaf, canopy and regional scales. *Agric. For. Meteorol.* **73**, 151–179 (1995).
53. Paulson, C. A. The mathematical representation of wind speed and temperature profiles in the unstable atmospheric surface layer. *J. Appl. Meteorol. Climatol.* **9**, 857–861 (1970).
54. Holtslag, A. & De Bruin, H. Applied modeling of the nighttime surface energy balance over land. *J. Appl. Meteorol. Climatol.* **27**, 689–704 (1988).
55. Culf, A. D. Equilibrium evaporation beneath a growing convective boundary layer. *Boundary Layer Meteorol.* **70**, 37–49 (1994).

56. Raupach, M. Combination theory and equilibrium evaporation. *Q. J. R. Meteorol. Soc.* **127**, 1149–1181 (2001).

Acknowledgements

L.R.V.Z. thanks the James S. McDonnell Foundation and the Harvard Center for the Environment for support. K.A.M. acknowledges funding from NSF grant no. AGS-2129576, a Sloan Research Fellowship and the Dean's Competitive Fund for Promising Scholarship from Harvard University. This work used samples from the traditional lands of the Newe (Western Shoshone) and Goshute peoples. A. Perelet and E. Kipnis provided laboratory assistance for this research. We thank E. Pardyjak and A. Perelet for their analytical assistance. We thank D. Bowling and H. Holmes for sharing their equipment with us. We thank C. A. Garcia for providing the data from the Nevada salt flats. This work was made possible with the support of former BLM West Desert District office staff, including K. Oliver, M. Preston, M. Nelson, C. Johnson, S. Allen, R. Draper, B. White and R. Tea. An NSF Coupled Natural Human Systems Award (no. 1617473) to B.B.B. and a University of Utah Global Change and Sustainability Center Graduate Student Research Grant funded this research. We thank E. Weeks and J. Henry for performing preliminary analyses.

Author contributions

K.A.M. proposed using salt flat data to address the study's main question. L.R.V.Z. and K.A.M. designed the research. L.R.V.Z. led the analysis, with contributions from K.A.M. and L.I.T. L.R.V.Z. wrote the first draft, with contributions from K.A.M. J.A.B. and B.B.B. provided the data for the Bonneville salt flats and aided observational analysis. L.R.V.Z., K.A.M., J.A.B., B.B.B., L.I.T., N.M.H., P.G. and P.H. contributed to writing and editing the manuscript.

Competing interests

The authors declare no competing interests.

Additional information

Supplementary information The online version contains supplementary material available at https://doi.org/10.1038/s44221-023-00147-9.

Correspondence and requests for materials should be addressed to Lucas R. Vargas Zeppetello or Kaighin A. McColl.

Peer review information *Nature Water* thanks Lucas Cernusak, Russell Scott and the other, anonymous, reviewer(s) for their contribution to the peer review of this work.

nature portfolio

Corresponding author(s): Vargas Zeppetello, L.R., McColl, K.A.

Last updated by author(s): Sep 14, 2023

Reporting Summary

Nature Portfolio wishes to improve the reproducibility of the work that we publish. This form provides structure for consistency and transparency in reporting. For further information on Nature Portfolio policies, see our Editorial Policies and the Editorial Policy Checklist.

Statistics

For all statistical analyses, confirm that the following items are present in the figure legend, table legend, main text, or Methods section.

n/a	Confirmed
☐	☒ The exact sample size (*n*) for each experimental group/condition, given as a discrete number and unit of measurement
☐	☒ A statement on whether measurements were taken from distinct samples or whether the same sample was measured repeatedly
☐	☒ The statistical test(s) used AND whether they are one- or two-sided *Only common tests should be described solely by name; describe more complex techniques in the Methods section.*
☐	☒ A description of all covariates tested
☐	☒ A description of any assumptions or corrections, such as tests of normality and adjustment for multiple comparisons
☐	☒ A full description of the statistical parameters including central tendency (e.g. means) or other basic estimates (e.g. regression coefficient) AND variation (e.g. standard deviation) or associated estimates of uncertainty (e.g. confidence intervals)
☐	☒ For null hypothesis testing, the test statistic (e.g. *F*, *t*, *r*) with confidence intervals, effect sizes, degrees of freedom and *P* value noted *Give P values as exact values whenever suitable.*
☒	☐ For Bayesian analysis, information on the choice of priors and Markov chain Monte Carlo settings
☒	☐ For hierarchical and complex designs, identification of the appropriate level for tests and full reporting of outcomes
☐	☒ Estimates of effect sizes (e.g. Cohen's *d*, Pearson's *r*), indicating how they were calculated

Our web collection on statistics for biologists contains articles on many of the points above.

Software and code

Policy information about availability of computer code

Data collection	No custom code was used to collect data in this study.
Data analysis	Python code used to analyze data in this study is available at https://github.com/Lvargaszeppetello/Surface_Conductance.

For manuscripts utilizing custom algorithms or software that are central to the research but not yet described in published literature, software must be made available to editors and reviewers. We strongly encourage code deposition in a community repository (e.g. GitHub). See the Nature Portfolio guidelines for submitting code & software for further information.

Data

Policy information about availability of data

All manuscripts must include a data availability statement. This statement should provide the following information, where applicable:

- Accession codes, unique identifiers, or web links for publicly available datasets
- A description of any restrictions on data availability
- For clinical datasets or third party data, please ensure that the statement adheres to our policy

The Bonneville data set analysed in the current study is available at https://github.com/Lvargaszeppetello/Surface_Conductance. The Dixie Valley salt flat data is available online at https://waterdata.usgs.gov/monitoring-location/394508118025505/#parameterCode=62968&startDT=2009-05-01&endDT=2010-05-01 and https://waterdata.usgs.gov/monitoring-location/394559118013705/#parameterCode=62968&startDT=2009-05-01&endDT=2010-05-01

Human research participants

Policy information about studies involving human research participants and Sex and Gender in Research.

Reporting on sex and gender	N/A
Population characteristics	N/A
Recruitment	N/A
Ethics oversight	N/A

Note that full information on the approval of the study protocol must also be provided in the manuscript.

Field-specific reporting

Please select the one below that is the best fit for your research. If you are not sure, read the appropriate sections before making your selection.

☐ Life sciences ☐ Behavioural & social sciences ☒ Ecological, evolutionary & environmental sciences

For a reference copy of the document with all sections, see nature.com/documents/nr-reporting-summary-flat.pdf

Ecological, evolutionary & environmental sciences study design

All studies must disclose on these points even when the disclosure is negative.

Study description	We used data from salt flats to understand variations in surface conductance in response to changes in soil moisture and vapor pressure deficit.
Research sample	Eddy flux covariance data from three salt flats.
Sampling strategy	All data that fit certain background environmental conditions described in the methods section were used in this study.
Data collection	Data were collected from eddy flux covariance towers.
Timing and spatial scale	Flux tower data are averaged at half-hour timescales.
Data exclusions	We excluded nighttime conditions, and situations where the eddy flux tower data are inconsistent with basic surface energy balance.
Reproducibility	All data and analysis code are available online.
Randomization	In one section, we used a random number generator from python to generate random numbers. Parameters for these values are described in the methods.
Blinding	Blinding is not relevant to this study.

Did the study involve field work? ☐ Yes ☒ No

Reporting for specific materials, systems and methods

We require information from authors about some types of materials, experimental systems and methods used in many studies. Here, indicate whether each material, system or method listed is relevant to your study. If you are not sure if a list item applies to your research, read the appropriate section before selecting a response.

Materials & experimental systems

n/a	Involved in the study
☒	☐ Antibodies
☒	☐ Eukaryotic cell lines
☒	☐ Palaeontology and archaeology
☒	☐ Animals and other organisms
☒	☐ Clinical data
☒	☐ Dual use research of concern

Methods

n/a	Involved in the study
☒	☐ ChIP-seq
☒	☐ Flow cytometry
☒	☐ MRI-based neuroimaging